Stepped Circular Waveguide Dual-Mode Filters for Broadband Contiguous Multiplexers

Hai Hu, *Student Member, IEEE*, Ke-Li Wu, *Fellow, IEEE*, and Richard J. Cameron, *Fellow, IEEE*

***Abstract*—A stepped circular waveguide dual-mode (SCWDM) filter is fully investigated in this paper, from its basic characteristic to design formula. As compared to a conventional circular waveguide dual-mode (CWDM) filter, it provides more freedoms for shifting and suppressing the spurious modes in a wide frequency band. This useful attribute can be used for a broadband waveguide contiguous output multiplexer (OMUX) in satellite payloads. The scaling factor for relating coupling value M to its corresponding impedance inverter K in a stepped cavity is derived for full-wave EM design. To validate the design technique, four design examples are presented. One challenging example is a wideband 17-channel Ku-band contiguous multiplexer with two SCWDM channel filters. A triplexer hardware covering the same included bandwidth is also designed and measured. The measurement results show excellent agreement with those of the theoretical EM designs, justifying the effectiveness of full-wave EM modal analysis. Comparing to the best possible design of conventional CWDM filters, at least 30% more spurious-free range in both Ku-band and C-band can be achieved by using SCWDM filters.**

***Index Terms*—Dual-mode waveguide filters, contiguous multiplexers.**

I. Introduction

A CONTIGUOUS channel waveguide output multiplexer (OMUX) is a core subsystem in communication satellite payloads. A typical OMUX comprises a number of waveguide channel filters connected to a waveguide manifold [1]. The circular waveguide dual-mode (CWDM) filter, amongst other filter technologies, has been the most preferred choice for the channel filters by virtue of its excellent power-handling capability, convenient coupling arrangements, relatively compact size, and its ability to realize advanced transfer characteristics since 1970s [2], [3].

In recent years, the rapidly-growing demand for service capacity has led to the needs for OMUXs with greater numbers of channels and wider working bandwidths. For such applications new challenges must be confronted in order to build a wideband contiguous OMUX [4]. One of the issues that must be solved is how to clean up the spurious resonances of a channel filter that interfere with the performance of other channel filters in the frequency band of interest. It will be shown in this paper that a stepped circular waveguide dual-mode (SCWDM) cavity filter can effectively provide a wide spurious-free band.

Manuscript received August 02, 2012; revised October 24, 2012; accepted October 26, 2012. Date of publication December 20, 2012; date of current version January 17, 2013. This work was supported by University Grants Committee of the Hong Kong Special Administrative Region under Grant AoE/P-04/08.

H. Hu and K.-L. Wu are with the Department of Electronic Engineering, The Chinese University of HK, Shatin, NT, Hong Kong (e-mail: hhu@ee.cuhk.edu.hk; klwu@ee.cuhk.edu.hk).

R. J. Cameron is with Canopus Consultancy, High Wycombe, Bucks, HP13 6QG, U.K. (e-mail: richard.cameron@ieee.org).

Color versions of one or more of the figures in this paper are available online at http://ieeexplore.ieee.org.

Digital Object Identifier 10.1109/TMTT.2012.2227787

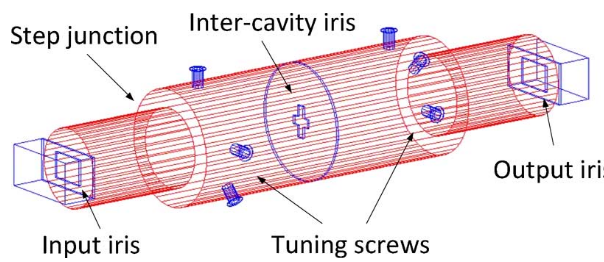

Fig. 1. Physical model of a Ku-band 4th-order SCWDM filter.

A typical 4-pole SCWDM filter is shown in Fig. 1. The functions of the coupling irises and tuning elements in an SCWDM filter are similar to those of a conventional CWDM filter. The only difference is that each cavity of an SCWDM filter consists of two different circular waveguides conjoined by a step junction. To explore the useful features of an SCWDM filter for broadband OMUX applications, three most concerned issues are studied, which are (1) to find a method that can quickly generate an approximated mode chart for prediction of the higher-order spurious resonances; (2) to develop a systematic electromagnetic (EM) design procedure of SCWDM channel filters and consequently a completely EM multiplexer, with which all the potential spurious modes can be accurately predicted prior to manufacturing; and (3) to experimentally verify the design procedure.

In order to develop an EM design procedure, one must understand the mode chart of the higher-order mode resonances of an SCWDM cavity. Unlike a uniform CWDM cavity, there is no analytical formula to determine the resonance frequency for each mode in a stepped cavity. When coming to the full-wave EM design of an SCWDM filter, the scaling factor of a coupling value M to its corresponding impedance inverter K in a stepped cavity must be derived. In this connection, the traditional CWDM filter design theory [5]–[9] may not be directly applied to the design of an SCWDM filter.

In this paper, a coarse but quick approach for generating the mode chart of an SCWDM cavity is developed. A systematic direct design procedure is presented, for which the formula of the scaling factor between the inverter parameter K and the coupling value M for an SCWDM filter is derived. To demonstrate the usefulness and effectiveness of the concept, four design examples are presented. The first example is the full-wave EM design of a Ku-band SCWDM filter; its designed responses are compared with the measured data of a prototype hardware. Based on an intensive study of the spurious modes behavior in Ku-band, a wideband 17-channel contiguous OMUX is designed by a full-wave EM modal analysis tool, in which the

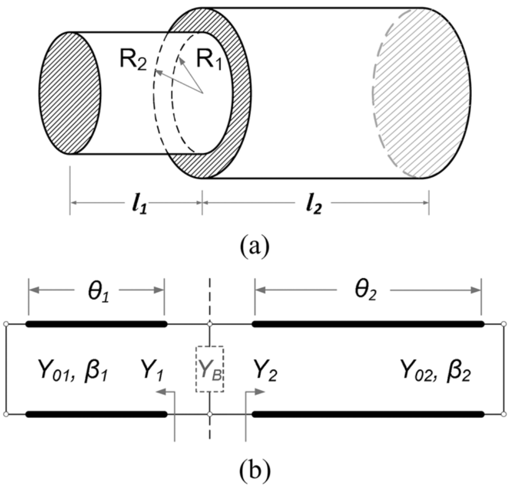

Fig. 2. SCWDM cavity: (a) the physical structure, and (b) the equivalent circuit model (with Y_B neglected in calculation) for approximately generating the mode chart.

two lowest frequency channels are realized by SCWDM filters for their wider spurious-free bands. This design is experimentally verified in the third design example: a triplexer (with one SCWDM channel filter) that covers exactly the same 1 GHz frequency range as that in the 17-channel OMUX case. A C-band design example is also examined, further confirmed that a wide spurious resonance clean frequency band can be created by appropriately choosing the diameters of an SCWDM cavity.

II. The Mode Chart of an SCWDM Cavity

An SCWDM cavity is illustrated in Fig. 2(a), where (l_1, R_1) and (l_2, R_2) are the lengths and radii for the small and large radius sections, respectively. With appropriate combination of (l_1, R_1) and (l_2, R_2), the spurious resonances in a frequency band can be moved away. This feature can be best viewed by the mode chart of the SCWDM cavity, which may be effectively used for characterizing the resonance frequencies of various modes and choosing the optimum combination of (l_1, R_1) and (l_2, R_2).

An approximate but efficient transmission line model is developed for generating the mode chart of an SCWDM cavity. As shown in Fig. 2(b), an SCWDM cavity can be described by an equivalent circuit of two short-circuited transmission lines with different characteristic admittances. The parameters $(Y_{01}, \beta_1, \theta_1)$ and $(Y_{02}, \beta_2, \theta_2)$ are the characteristic admittance, propagating constant and the electrical length for the waveguide mode considered (e.g., TE_{11}) in the small and large radius sections, respectively. The shunt susceptance Y_B accounts for the higher order mode effect of the step discontinuity, which is frequency and mode dependant and thus is difficult to be modeled by a closed-form expression.

When a chosen mode in an SCWDM cavity resonates, the total admittance of the mode at the step junction must equal to zero, that is

$$Y_1 + Y_2 + Y_B = 0. \tag{1}$$

Usually, the selected radius ratio (R_1/R_2) of the two waveguides is not smaller than 0.75, the effect of Y_B is not significant and thus will be neglected in the approximated mode chart calculations. It will be shown later that the maximum relative discrepancy in the calculated resonance frequencies by the approximated transmission line model with Y_B omitted and rigorous full wave EM model is less than 6% in C band for the case of $R_1/R_2 = 0.75$. Substituting the admittance expressions of each mode in the two pieces of short-circuited transmission lines for Y_1 and Y_2 into (1), the resonances of the mode in an SCWDM cavity are then approximately governed by

$$Y_{01}/\tan\theta_1 + Y_{02}/\tan\theta_2 = 0 \tag{2}$$

where $\theta_1 = \beta_1 l_1, \theta_2 = \beta_2 l_2$. Even though the characteristic admittance (Y_{01} and Y_{02}) for a waveguide mode is not uniquely defined, its frequency dependence is the same as that of its wave impedance. Thus the transcendental equation (2) leads to a set of unique resonance frequencies for each mode. For any given R_1 and R_2, the change of θ_1 or θ_2 will lead to the change of resonance frequencies, collecting all these frequencies generates the mode chart for the particular mode.

The resonances of an SCWDM cavity can also be rigorously analyzed by a full-wave EM simulation using an eigen solver. The full-wave generated mode chart has been used to cross-check the approximated results.

In practice, the working mode in an SCWDM cavity resonates near the filter center frequency f_0. Therefore, when sweeping the θ_1 for making a mode chart, the electrical length of the cavity, i.e., $\theta_1 + \theta_2$, needs to be kept at $k\pi$ for TE_{11k} resonance To demonstrate, the mode chart of a C-band SCWDM cavity with $R_1 = 30.0$ mm and $R_2 = 40.0$ mm is shown in Fig. 3, where the x-axis is the electrical length θ_1 of TE_{11} mode in the smaller radius section and the y-axis is the resonance frequencies of the modes in the cavity. The solid lines are generated by the approximated approach while the dashed lines are by a full-wave EM approach. In this example $\theta_1 + \theta_2$ is fixed to π for TE_{111} mode resonating near $f_0 = 3.46$ GHz. For θ_1 equals 0 and π, the frequencies represent the resonance frequencies for the uniform cavities with radius of $R = 40.0$ mm and $R = 30.0$ mm, respectively. It can be seen from Fig. 3 that even though there are some discrepancies between the two sets of curves, the mode chart generated by the approximated model is good enough for a fast engineering design.

The mode chart in a Ku-band SCWDM cavity, whose $R_1 = 12.0$ mm and $R_2 = 15.0$ mm, is also generated and is given in Fig. 4. This SCWDM cavity is for realizing the channel filter of the lowest frequency channel of a wideband OMUX ranging from 10.6 GHz to 11.8 GHz. The f_0 of the filter is 10.73 GHz. By sweeping θ_1 from 0 to 3π, one can find that when θ_1 is at the vicinity of 1.0π, the spurious-free window is much expanded comparing to a uniform 3π long CWDM cavity with radius of either R_1 or R_2.

A spurious-free range of an SCWDM cavity also depends on the choices of radii R_1 and R_2. Since the approximated approach is very fast, it would be straightforward to generate a series of mode charts with different R_1 and R_2 combinations.

III. Design Theory of an SCWDM Filter

Due to the different termination conditions, the two degenerate TE_{11} modes, namely v and h modes (also known

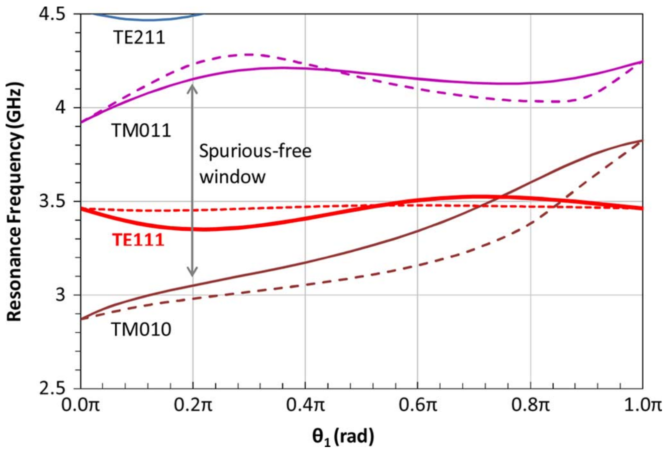

Fig. 3. The mode chart of a C-band SCWDM cavity with $R_1 = 30.0$ mm, $R_2 = 40.0$ mm, and $\theta_1 + \theta_2$ is fixed to π for TE_{111} resonating near $f_0 = 3.46$ GHz. The solid lines are generated by the approximated approach, while the dashed lines are by a full-wave eigen analysis approach.

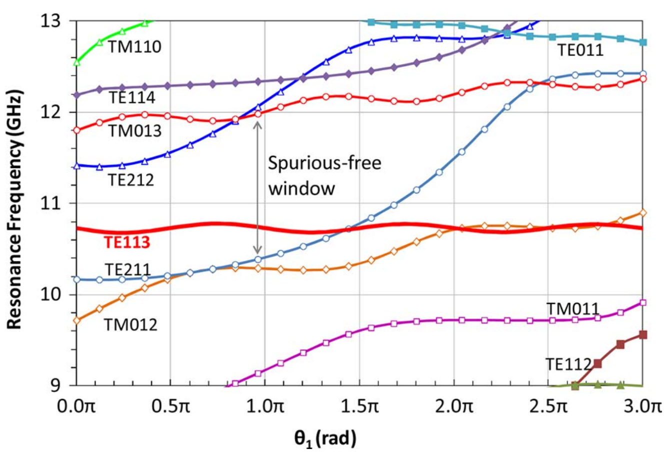

Fig. 4. The mode chart of a Ku-band SCWDM cavity with $R_1 = 12.0$ mm, $R_2 = 15.0$ mm, and $\theta_1 + \theta_2$ is fixed to 3π for TE_{113} resonating near $f_0 = 10.73$ GHz.

as $\mathrm{TE}_{11\,\cos}$ and $\mathrm{TE}_{11\,\sin}$ modes), resonating in a $k\pi$ electrical-long cavity will have different degrees of phase offsets. The design process comprises four steps: 1) choose an appropriate set of (θ_1, R_1) and (θ_2, R_2) from the mode chart presented, so that the SCWDM filter can shift the spurious modes to unused frequency bands; 2) determine the position of the screws for degenerate mode coupling; 3) design coupling elements according to the prescribed coupling values; and 4) tune the tuning screws and determine cavity lengths at which the overall phases of the two degenerate modes in each cavity is balanced [7], [9].

A. The Scaling Factor Between M and K

Each coupling iris and coupling screw is designed using the concept of impedance inverter, which is a key parameter of the distributed circuit model. To ensure the slopes of the resonance admittances of the distributed element circuit model and the coupling matrix (lumped element circuit) model equal, the coupling matrix needs to be scaled [10].

The distributed element model of an SCWDM cavity can be represented by two cascaded waveguide segments, while the

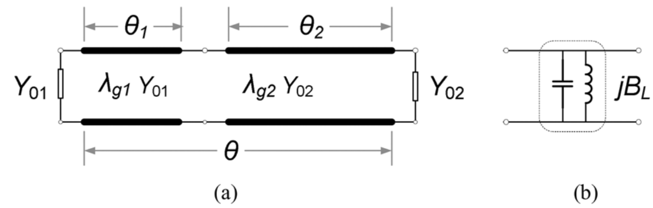

Fig. 5. Two SCWDM resonator presentations: (a) the distributed element circuit model, and (b) the lumped element circuit model.

lumped element model is represented by an LC resonator. The two circuit models are shown in Fig. 5, where λ_{g1} and λ_{g2} in Fig. 5(a) are the frequency-dependent waveguide wavelengths in the small and large radius sections of an SCWDM cavity.

After normalizing to their characteristic admittances, the normalized resonance admittances B_D and B_L for the distributed and lumped resonator models are expressed in (3) and (4) below, respectively:

$$jB_D = j\sin(\theta_1 + \theta_2) + j\frac{\lambda_{g2} - \lambda_{g1}}{\lambda_{g01} + \lambda_{g02}}\sin(\theta_1 - \theta_2) \quad (3)$$

$$jB_L = j\left(\frac{\omega}{\omega_0} - \frac{\omega_0}{\omega}\right), \quad (4)$$

where ω is angular frequency, $\omega_0 = 2\pi f_0$, $\lambda_{g01} = \lambda_{g1}(\omega_0)$ and $\lambda_{g02} = \lambda_{g2}(\omega_0)$. The second term of (3) can be considerably small if the stepped cavity radii ratio R_1/R_2 is larger than 0.75, thus it is neglected in the followed slope scaling factor calculation.

To obtain the scaling factor between the two models shown in Fig. 5, both the values and the slopes for B_D and B_L must be matched at ω_0. The slope of B_L at ω_0 is calculated by:

$$S_L = \left.\frac{dB_L}{d\omega}\right|_{\omega=\omega_0} = \frac{2}{\omega_0}. \quad (5)$$

Similarly, the slope S_D for B_D at ω_0 can also be calculated. The scaling factor is then defined by

$$S_F = \frac{S_D}{S_L} \approx \frac{1}{2}\left(\left(\frac{\lambda_{g01}}{\lambda_0}\right)^2\theta_1 + \left(\frac{\lambda_{g02}}{\lambda_0}\right)^2\theta_2\right) \quad (6)$$

where λ_0 is free space wavelength at ω_0.

It can be derived that the filter input/output coupling coefficient $M_{\mathrm{I/O}}$ is scaled to the inverter parameter K by:

$$K = M_{\mathrm{I/O}}\sqrt{S_F\Omega} \quad (7)$$

where $\Omega = \mathrm{BW}/f_0$, is the fractional bandwidth of the filter. Similarly, a non I/O coupling M_{INT} is scaled to the inverter parameter$K$ by:

$$K = M_{\mathrm{INT}}S_F\Omega. \quad (8)$$

The expressions for (7) and (8) are also given in [12].

With the above analytical relations, the filter lumped element circuit model described by a coupling matrix can be easily associated to its corresponding distributed circuit model, which is described by the S-parameters of each coupling discontinuity at the center frequency.

B. Calculation of Couplings

An input/output iris couples energy from the TE_{10} mode in the rectangular waveguide to the v mode in the circular waveguide. In calculating the I/O coupling of an SCWDM filter, the input iris should also include the section of small radius cavity and the step discontinuity. The K impedance inverter [5]–[10] is used for determining the coupling $M_{\mathrm{I/O}}$ (e.g., M_{01} and M_{45} for a 4-pole filter) and reflection phases $\varphi_{\mathrm{vI/O}}$ and $\varphi_{\mathrm{hI/O}}$ looking at the I/O iris from the large radius cavity. The reflection phase is an extra amount of phase introduced by an iris if compared to a perfect electric conducting wall. It should be noted that the effect of electrical length θ_1 has been taken into account in the reflection phases. Equation (7) will be used to scale the inverter parameter K to the corresponding coupling $M_{\mathrm{I/O}}$.

The irises for inter-cavity couplings can be in rectangular or cruciform shape, depending on the coupling topology. The conventional T-network model for K impedance inverter can be used for determining the coupling value M_{INT} (e.g., M_{23} and M_{14} for a 4-pole filter) and the reflection phases φ_{vINT} and φ_{hINT} simultaneously [5]–[9]. The inverter parameter K is scaled to its coupling M_{INT} by (8).

Calculating the coupling between two degenerate modes in the cavity (e.g., M_{12} and M_{34} for a 4-pole filter) is not as straightforward as the calculation of an iris coupling because it involves the interactions between v, h modes and all the higher order modes. A generalized K inverter model that is described by the generalized scattering matrix (GSM) of the screw section at the filter center frequency can be used to approximately model the coupling of the v and h modes in an SCWDM cavity [7], [9]. The obtained inverter parameter K is also scaled to its coupling M by (8).

C. Phases Balance in a Dual-Mode Cavity

Balancing the phases of the two degenerate modes in an SCWDM cavity includes: 1) realizing the required v and h mode frequency offsets (self-couplings); 2) determining the physical position of the tuning and coupling element for the degenerate modes; and 3) calculating the cavity length.

For an asynchronously-tuned SCWDM filter, the relationship between the frequency shifts and the corresponding phase offsets (φ_{vS} and φ_{hS}) of the degenerate TE_{11k} modes can be found by perturbing the phase with respect to the frequency change for a given cavity length at the center frequency. The extra phases caused by self-couplings are usually compensated by the tuning screws.

Having designed each coupling iris, when the total phase of v mode equals to that of h mode, the following phase balance condition should be fulfilled:

$$\varphi_{\mathrm{vI/O}} + \varphi_{\mathrm{vM}} + \varphi_{\mathrm{vINT}} + \varphi_{\mathrm{vS}} = \varphi_{\mathrm{hI/O}} + \varphi_{\mathrm{hM}} + \varphi_{\mathrm{hINT}} + \varphi_{\mathrm{hS}} \tag{9}$$

which is equal to $\Delta\varphi$. The main cavity length is determined thereafter by $k\pi - \Delta\varphi$.

The physical position φ_{S} of the screw section can be found by

$$\varphi_{\mathrm{S}} = (k\pi - \Delta\varphi - \varphi_{\mathrm{hINT}} - \varphi_{\mathrm{vINT}})/2 \tag{10}$$

TABLE I
COUPLING MATRIX FOR THE KU-BAND SCWDM FILTER

M_{01}	1.0628	M_{14}	-0.2946	M_{34}	0.8797
M_{12}	0.8797	M_{23}	0.8333	M_{45}	1.0628

where φ_{S} is measured from the inter-cavity iris interface plane to the screw section interface plane, and then the screws are very closely positioned to the maximum of electrical field along the axis direction.

IV. DESIGN EXAMPLES

Four design examples are presented in this section. The full-wave EM simulation for all the examples is performed by an in-house modal analysis program, and is cross-checked by the commercial software μWave Wizard [11]. Nearly identical results are achieved. Besides, a small amount of eccentricity to each iris (with respect to the axial center of the connecting waveguide) is deliberately introduced in full-wave EM modal analysis to imitate the mechanical manufacture asymmetries, which will excite spurious modes.

Design Example 1: Design of a Ku-Band SCWDM Filter: This Ku-band filter example is designed and experimentally investigated for preparing the lowest-frequency channel of a wideband OMUX, which will be shown in design example 2 and 3. The design specifications for the 4-th order filter are: $f_0 = 10.73$ GHz, BW $= 54$ MHz with a 22 dB equal-ripple return loss. A very wide spurious-free window from 10.6 GHz to 11.8 GHz is required. The synthesized coupling matrix is listed in Table I. The filter will be designed with two circular waveguide cavities of electrical length 3π and is interfaced with WR75 rectangular waveguide at the input and output.

A series of conventional CWDM filters with radii ranging from 9.5 mm to 15 mm were designed first. The full-wave EM responses of the designed filters are compared in Fig. 6, where the Spurious Resonances (SR) are marked beside the spikes with the cavity radius (in mm) denoted as the subscripts. It can be clearly observed that all these conventional CWDM filters fail to meet the out-of-band spurious-free requirement.

For comparison purpose, an SCWDM filter is then designed. Before designing a complete SCWDM filter, mode charts need to be made to search for the dimension of an optimal SCWDM cavity. From the mode chart shown in Fig. 4, the selection of $R_1 = 12.0$ mm and $\theta_1 = 0.95\pi$ for the stepped waveguide section and $R_2 = 15.0$ mm for the main cavity will provide a sufficiently wide spurious-free range. The SCWDM filter is designed by following the aforementioned design process. The EM simulated transmission coefficient of the SCWDM filter is superimposed in Fig. 6 by a dotted line. As indicated by the mode chart, the designed SCWDM filter does provide a spurious-free band from 10.5 to 12 GHz.

To verify the full-wave EM model, an SCWDM filter hardware is also manufactured and tested. The filter physical dimensions are as follows: the lengths of the small and large radius waveguide sections are 18.0 mm and 33.2 mm, respectively; the thickness of all the irises is 0.5 mm; the aperture of the I/O irises is 8.8 × 8.0 mm; the cruciform inter-cavity iris is 5.8 × 7.8 mm in outer dimension, and 2.0 mm for the slot width; the diameter of all the tuning screws is 3.0 mm.

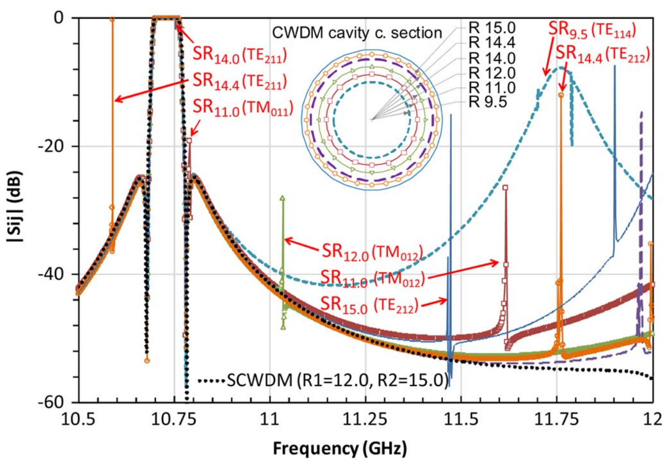

Fig. 6. Full-wave EM simulated wide band characteristics of a series of conventional Ku band CWDM filters and an SCWDM filter. All dimensions are in mm.

The narrow-band responses from the circuit model, the full-wave EM model and the hardware measurement are compared in Fig. 7(a). It can be seen that the responses of the three models agree very well. From the in-band insertion loss curve as presented in Fig. 7(a), the extracted unloaded Q-factor of the filter is 12800, which is the same as the full-wave model prediction if a conductivity of $\sigma = 3.0 \times 10^7$ S/m is assumed. As a reference, with the same σ, the unloaded Q for a full-wave designed conventional CWDM filter with $R = 12$ mm and $R = 15$ mm are 11500 and 14000, respectively.

The broadband performance of the EM model and the hardware is shown in Fig. 7(b). The measurement result has confirmed the 10.5 GHz to 12 GHz spurious-free range of the designed SCWDM filter, which is about 35% wider than the best conventional CWDM filter design that is with $R = 14.4$ mm providing a 1.1 GHz spurious-free range. Moreover, the spurious resonance spikes predicted by the full-wave EM model perfectly match those of the measured data, justifying that the full-wave EM modal analysis is competent for such study.

Design Example 2: A 17-Channel Ku-Band Contiguous OMUX: The frequency range for a 17-channel Ku-band OMUX is set from 10.7 GHz to 11.72 GHz, with 54 MHz usable bandwidth for each channel. The OMUX is to be designed with a WR75 manifold in the 'fishbone' topology [1].

The circuit model is designed and optimized first to achieve a contiguous 22 dB common port return loss. In order to EM design such a wide-band OMUX, as is already presented in design example 1, a few of SCWDM filters need to be used for the lower band channels, specifically, channels CH01 and CH02. Both SCWDM filters are designed with $R_1 = 12.0$ mm, $\theta_1 = 0.95\pi$ and $R_2 = 15.0$ mm. The rest of the channel filters are realized by conventional CWDM filters with $R = 14.4$ mm.

The coupling matrices for all the channel filters are firstly synthesized [1]. All the channel filters are then EM designed independently one by one. Having had channel filters designed and the phase-loading [13] removed, they are assembled onto the manifold through E-plane T-junctions. The final physical structure of the 17-channel OMUX is illustrated in Fig. 8, where the waveguide shortend, the common port and channel sequences are indicated. A 15 dB or better common port return loss can be achieved before any fine tuning. With minor adjustment of the manifolds lengths alone, the return loss can be easily pushed down to 20 dB in this example. The EM simulated responses of the adjusted OMUX design are shown in Fig. 9.

Design Example 3: A Ku-Band Triplexer With 1 GHz Included Bandwidth: Since it is too expensive to hardware proto-

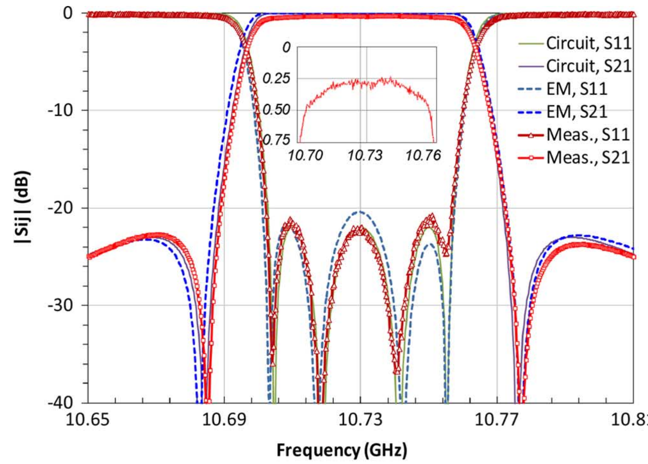

(a)

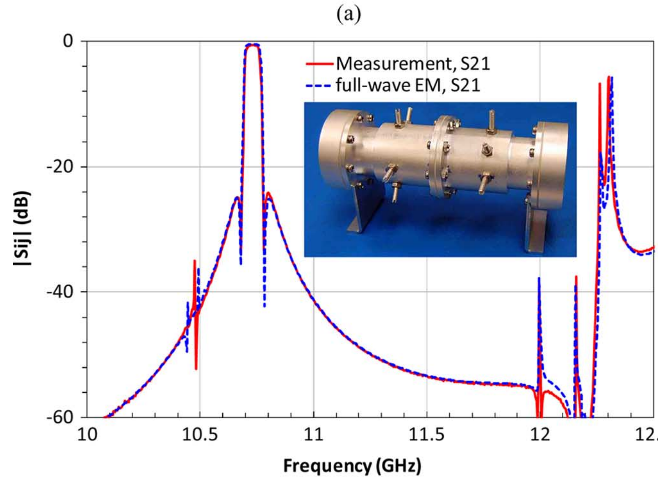

(b)

Fig. 7. The Ku-band SCWDM filter: (a) narrowband S-parameters of the circuit model, full-wave EM model and measurement, and (b) broadband S-parameters of the full-wave EM model and the measurement.

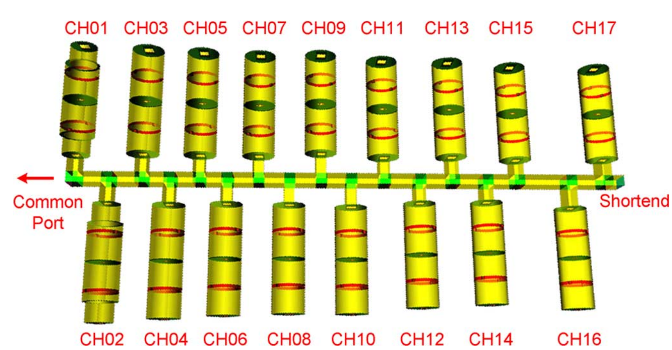

Fig. 8. The 17-channel contiguous OMUX: the topology illustration, with CH01 and CH02 realized by SCWDM filters and other channels by CWDM filters.

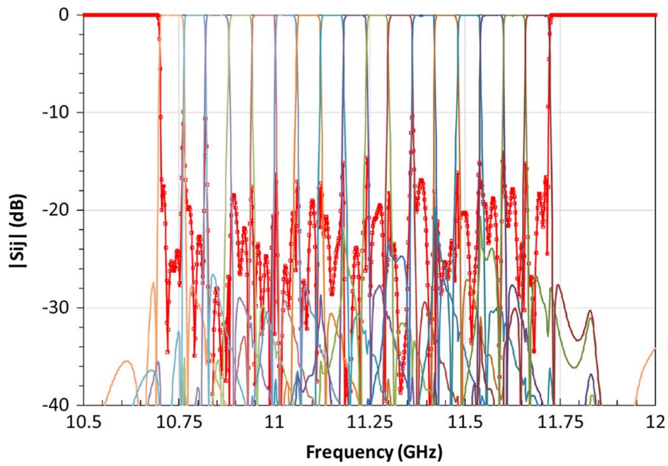

Fig. 9. 17-channel contiguous OMUX: S-parameters from EM modal analysis.

type the OMUX in design example 2, a triplexer that includes exactly the same included bandwidth as that of example 2 is designed and manufactured instead. This example can experimentally demonstrate the effectiveness of a SCWDM filter for a wide-band OMUX design.

The center frequencies of the triplexer channel filters (namely CH01, CH02 and CH03) are 10.73 GHz, 11.63 GHz and 11.69 GHz, which are deliberately chosen to be the same as those of channel CH01, CH16 and CH17 of the 17-Channel OMUX in design example 2, respectively. The bandwidth for each channel is also 54 MHz. The lowest frequency channel, i.e., CH01, adopts SCWDM filter with the same cavity dimensions as that in examples 1 and 2. The other two channels use conventional CWDM filters with $R = 14.4$ mm.

The triplexer is full-wave EM designed according to a pre-synthesized circuit model. The hardware of the three channel filters are then built and tuned according to the designed circuit model. The final manifold-coupled triplexer hardware is shown in Fig. 10(a) with channel sequences marked. The broadband responses of the prototyped hardware and the full-wave EM model are compared in Fig. 10(b), where the shaded part denotes the total included bandwidth of the triplexer. It can be seen a 1.5 GHz spurious-free window has been achieved. Furthermore, the spurious resonance spikes predicted by full-wave EM model are reasonably accurate as comparing to the measurement result.

Design Example 4: A C-Band SCWDM Filter: A C-band SCWDM filter is demonstrated through an EM designed model in this example. The filter design specifications are: $f_0 = 3.46$ GHz, $\mathrm{BW} = 36$ MHz with a 20 dB equal-ripple return loss. The coupling values for this example are shown in Table II. In this design TE_{111} mode is used. The two radii for the SCWDM cavity are $R_1 = 30$ mm and $R_2 = 40$ mm. Using the mode chart shown in Fig. 3, $\theta_1 = 0.2\pi$ is selected as the length for the stepped waveguide so that a wide spurious-free window can be created.

To show the effectiveness of the C-band SCWDM filter, three conventional CWDM filters with radii of 30.0, 35.0 and 40.0 mm are also designed. The full-wave EM responses of the designed SCWDM filter and those from the conventional CWDM filters are superimposed and are shown in Fig. 11 with spurious resonances (SR) markers. Obviously, the SCWDM filter in this

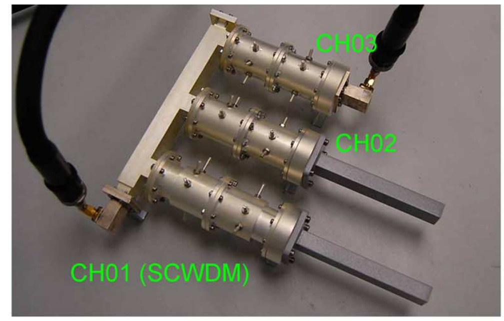

(a)

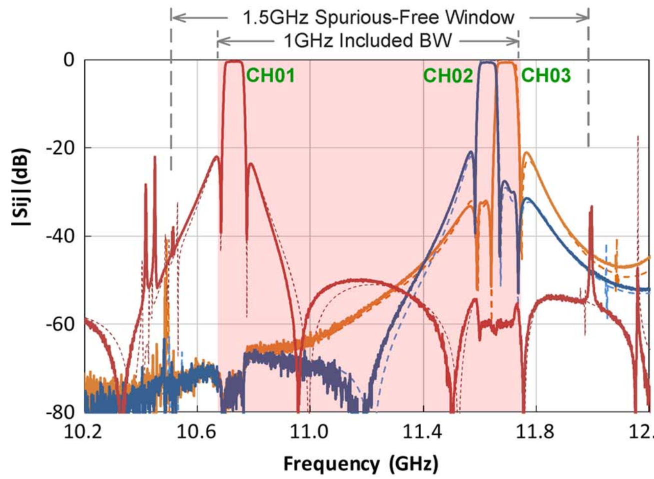

(b)

Fig. 10. The Ku-band triplexer with 1 GHz included bandwidth: (a) hardware photograph, and (b) the broadband rejection responses of measurement result (solid lines) and full-wave EM result (dashed lines).

TABLE II
COUPLING MATRIX FOR THE C-BAND SCWDM FILTER

M_{01}	1.0190	M_{14}	-0.2542	M_{34}	0.8450
M_{12}	0.8450	M_{23}	0.7990	M_{45}	1.0190

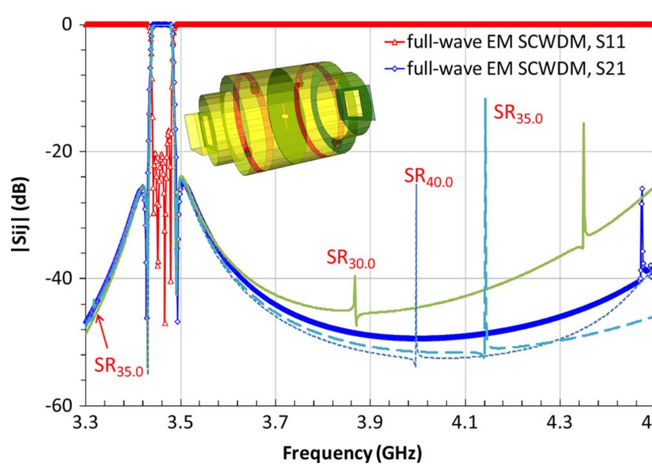

Fig. 11. Full-wave EM simulated wideband characteristics of a series of conventional C band CWDM filters and one SCWDM filter.

example outperforms the conventional CWDM filters in terms of spurious-free range.

V. CONCLUSION

The stepped circular waveguide dual-mode filter that can provide an excellent broadband spurious-free characteristic is investigated in this paper. An approximated but fast transmission line model for generating a mode chart of an SCWDM cavity is developed for quick engineering design. The scaling factor, which is a key relation in EM design procedure, between the lumped element circuit parameters and the distributed element circuit coefficients for an SCWDM filter has been derived. The usefulness of an SCWDM filter and the design formulae have been verified not only by EM models but also the solid hardware experiments. The attractive feature of potentially a wide spurious-free band for realizing a wideband OMUX is demonstrated through a full-wave EM design of a 17-channel Ku-band contiguous OMUX and a wideband triplexer hardware prototype. Comparing to the best possible design of conventional CWDM filters, at least an additional 30% spurious-free range in the Ku-band and C-band can be achieved.

References

[1] R. J. Cameron and M. Yu, "Design of manifold-coupled multiplexers," *IEEE Microw. Mag.*, vol. 8, no. 5, pp. 46–59, Oct. 2007.

[2] A. E. Atia and A. E. Williams, "New types of waveguide band-pass filters for satellite transponders," *Comsat Tech. Rev.*, vol. 1, no. 1, pp. 21–43, 1971, Fall.

[3] C. Kudsia, R. Cameron, and W.-C. Tang, "Innovations in microwave filters and multiplexing networks for communications satellite systems," *IEEE Trans. Microw. Theory Tech.*, vol. 40, pp. 1133–1149, Jun. 1992.

[4] M. Yu and Y. Wang, "Synthesis and beyond," *IEEE Microw. Mag.*, vol. 12, no. 6, pp. 62–76, Oct. 2011.

[5] J. R. Montejo-Garai and J. Zapata, "Full-wave design and realization of multicoupled dual-mode circular waveguide filters," *IEEE Trans. Microw.Theory Tech.*, vol. 43, pp. 1290–1297, Jun. 1995.

[6] M. Bekheit and S. Amari, "A direct design technique for dual-mode inline microwave bandpass filters," *IEEE Trans. Microw. Theory Tech.*, vol. 57, no. 9, pp. 2193–2202, Sep. 2009.

[7] K.-L. Wu, "An optimal circular waveguide dual-mode filter without tuning screws," *IEEE Trans. Microwave Theory Tech.*, vol. 47, no. 3, pp. 271–276, Mar. 1999.

[8] S. Cogollos, M. Brumos, V. E. Boria, C. Vicente, J. Gil, B. Gimeno, and M. Guglielmi, "A systematic design procedure of classical dual-mode circular waveguide filters using an equivalent distributed model," *IEEE Trans. Microw. Theory Tech.*, vol. 60, no. 1, pp. 1006–1017, Jan. 2012.

[9] H. Hu and K.-L. Wu, "An automated design technique for asynchronously-tuned circular waveguide dual-mode filters," in *Proc. Asia Pacific Microwave Conf.*, Yokohama, Japan, 2010, pp. 1970–1973.

[10] G. Matthaei, L. Young, and E. M. T. Jones, *Microwave Filters, Impedance Matching Networks and Coupling Structures*. Norwood, MA: Artech House, 1980.

[11] *μWave Wizard*. Bremen, Germany: Mician GmbH, v7.7.

[12] H. Hu, K.-L. Wu, and R. J. Cameron, "The design of stepped circular waveguide dual-mode filters for broadband contiguous multiplexers," in *Proc. IEEE Int. Microwave Symp.*, Baltimore, MD, Jun. 5–10, 2011, pp. 1–4.

[13] M. Meng and K.-L. Wu, "An analytical approach to computer-aided diagnosis and tuning of lossy microwave coupled resonator filters," *IEEE Trans. Microw. Theory Tech.*, vol. 57, no. 12, pp. 3188–3195, Dec. 2009.

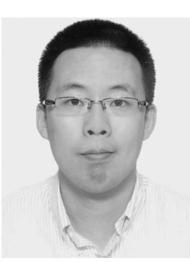

Hai Hu (S'10) received the B.Sc. degree from Nanjing University, Nanjing, China, in 2004, and the M.Phil. degree from the Chinese University of Hong Kong in 2006, both in electronic engineering.

From 2006 to 2010 he was a Research Assistant with the Department of Electronic Engineering, The Chinese University of Hong Kong, where his duty included the numerical modeling of LTCC layouts and passive integrated circuit components, automatic design of dual-mode waveguide filter and manifold multiplexer for payload systems. In 2010 he began to pursue a Ph.D. degree in the same institute. His research fields include non-planar filter, such as dielectric filter and compact multimode filter's design and application for next generation wireless base station systems; analytical computer-aided tuning (CAT) techniques; computational electromagnetic algorithms for modeling of waveguide structures; frequency and time-domain numerical modeling and analysis of multilayered high-speed RF circuits.

Mr. Hu was the recipient of 2012 Asia-Pacific Microwave Conference Prize.

Ke-Li Wu (M'90–SM'96–F'11) received the B.S. and M.Eng. degrees from the Nanjing University of Science and Technology, Nanjing, China, in 1982 and 1985, respectively, and the Ph.D. degree from Laval University, Quebec, QC, Canada, in 1989.

From 1989 to 1993, he was with the Communications Research Laboratory, McMaster University, as a Research Engineer and a Group Manager. In March 1993, he joined the Corporate R&D Division, COM DEV International, the largest Canadian space equipment manufacturer, where he was a Principal Member of Technical Staff. Since October 1999, he has been with The Chinese University of Hong Kong, Hong Kong, where he is a Professor and the Director of the Radiofrequency Radiation Research Laboratory (R3L). He has authored or coauthored numerous publications in the areas of EM modeling and microwave passive components, microwave filter and antenna engineering. His current research interests include PEEC and DPEC electromagnetic modeling of high speed circuits, RF and microwave passive circuits and systems, synthesis theory and practices of microwave filters, antennas for wireless terminals, LTCC-based multichip modules (MCMs), and RF identification (RFID) technologies. His research group is the main workforce in various active RFID research and applications in Hong Kong.

Prof. Wu is a member of IEEE MTT-8 subcommittee (Filters and Passive Components) and also serves as a TPC member for many prestigious international conferences including International Microwave Symposium. He was an Associate Editor of IEEE Transactions on Microwave Theory and Techniques from 2006 to 2009. He was the recipient of the 1998 COM DEV Achievement Award for the development of exact EM design software of microwave filters and multiplexers and Asia-Pacific Microwave Conference Prize in 2008 and 2012.

Richard J. Cameron (M'83–SM'94–F'02) received the B.Sc.degree in electronics with telecommunications at the University of Loughborough in 1969.

He subsequently joined the Marconi Space and Defence Company to begin a career devoted to the design and R&D of microwave equipment and systems for spacecraft and associated ground stations. In 1975 he joined The European Space Research and Technology Establishment (ESTEC), the technical branch of the European Space Agency (ESA) based in the Netherlands. Here he was involved in the development of software for the design of advanced microwave equipment for space application, particularly microwave filters. Since joining ComDev Ltd., Aylesbury, U.K., in 1984, he has been involved in the development of software and methods for the design of high performance microwave components and subsystems for both space and terrestrial application. He retired from ComDev in 2005, but retained a consultancy rôle with the Company on an *ad hoc* basis. Since retirement he has conducted several short lecture series for undergraduate and post-graduate students in Hong Kong and the U.K. He has also been appointed a Visiting Professor at the University of Leeds and as a Distinguished Microwave Lecturer for the 2013–15 term. During his career he has filed 8 patents and has authored or co-authored many papers for technical journals and conferences. He is also the co-author of a technical book *Microwave Filters for Communication Systems—Fundamentals, Design and Applications* (Wiley, 2007).